Loess particles loaded petaloid Bi_2S_3 nanowires for highly efficient photodegradation of dyesunder sunlight

Haiyan Yan, Qianqian Wang, Yufeng He*, Ya Shen, Pengfei Song & Rongmin Wang*

Key Laboratory of Eco-functional Polymer Materials of the Ministry of Education, College of Chemistry &
Chemical Engineering, Northwest Normal University, Lanzhou 730070, China

Email: heyufeng@nwnu.edu.cn/ wangrm@nwnu.edu.cn

In this paper, using loess particles (LoP), a kind of extremely common and inexpensive natural silicate particles with metastable structure, as inorganic carrier, the petaloid Bi_2S_3 nanowires have been loaded by in-situ depositing, which afforded loess particles loaded petaloid Bi_2S_3 nanowires (PBiNw@LoP) with one-step hydrothermal procedure. Scanning electron microscopy, Fourier transform infrared spectroscopy, X-ray diffraction, and adsorption-desorption isotherms of N_2 have been employed to characterize the prepared composite photocatalyst. The results show that the petaloid Bi_2S_3 nanowires are evenly dispersed on the loose surface of loess particles. The photocatalytic activity of PBiNw@LoP is evaluated by photodegradation of methylene blue (MB) irradiated with sunlight. It is demonstrated that PBiNw@LoP exhibits the superior photocatalytic performance with the photocatalytic degradation rate of 99.5%. The petaloid Bi_2S_3 nanowires with larger specific surface helps to absorb light, while the loose surface of loess with certain adsorption capacity. Therefore, the photocatalytic activity has been improved by the synergistic effect in photodegradation of dyes, while the ratio of Bi_2S_3 in catalyst is decreased without affecting the photodegradation performance. In conclusion, a cheap and efficient photocatalyst has been successfully prepared for the degradation of dye wastewater.

Keywords: Loess particles, Petaloid Bi_2S_3 nanowires, Photodegradation, Synergistic effect

With the development of industry, many rivers as well as lakes had been badly polluted, especially in developing countries[1,2], which directly affect the healthy drinking water of human beings. Therefore, many water treatment technologies, including physical and chemical treatment, were exploited for safe and efficient removing pollutants[3,4,5]. Especially, it is very important to remove dyes from industrial or domestic sewage systems before discharging into nearby water resources. In a variety of pollutant dyes, methylene blue (MB) is considered as a particularly hazardous pollutant due to its non-biodegradability and toxicity even at very low concentrations[6]. Among the solutions, semiconductor heterogeneous photocatalysis has become a potential solution to degrade virulent organic pollutants for environmental sustainability[7]. Photocatalysis is based upon the use of UV irradiated semiconductors, such as TiO_2, to eliminate various organic pollutants[8]. Numerous efforts have been made to improve the photocatalytic activity[9,10,11]. Since discovery of layered Bi_2S_3 nanomaterials[12], it has been paid attention in the fields of electrochemistry[13,14] and photocatalytic materials[15,16] as it can inhibit the recombination of photoelectron hole pairs that enhance the oxidation and reduction of nanoparticles[17]. However, one disadvantage of Bi_2S_3 nanomaterial is slight toxicity[18], and some kinds of Bi_2S_3 based composites of heterostructures had been prepared for improving their photocatalytic properties and toxicity[19,20,21]. In this paper, the loess particles (LoP), a kind of non-toxic, pollution-free and inexpensive natural silicate particles, was used as inorganic carrier, the petaloid Bi_2S_3 nanowires were loaded by in-situ depositing with one-step hydrothermal procedure, which afforded loess particles loaded petaloid Bi_2S_3 nanowires (PBiNw@LoP). After being characterized by SEM, FTIR, XRD, and adsorption-desorption isotherms of N_2, its photocatalytic degradation performance was investigated.

Materials and Methods

Loess was collected from the local hill near Lanzhou city of China. Bismuth chloride ($BiCl_3$) used in the experiments were purchased by Shanghai Macklin Biochemical Co. Ltd. Thiourea (CH_4N_2S) was obtained by Tianjin Chemical Reagent Factory. PVP-K30 (Shanghai Zhongqin Chemical Reagent

Co. Ltd.) and ethylene glycol (Tianjin Damao Chemical Reagents Factory) were obtained commercially. All reagents were used without further purification.

Separation of the small loess particles

In a beaker containing 400 mL of water,100 g dried loess powder was added and stirred for 12 h with a mechanical stirrer at room temperature until loess particles being dispersed completely. Firstly, after 2 min standing of the loess powder turbid solution, the supernatant suspension was quickly collected. Secondly, the obtained 300 mL of supernatant suspension was stirred for 20 min. Then, after standing for 10 min, the supernatant suspension was collected. Thirdly, the above 200 mL of supernatant suspension stood for 24 hrs. Then, the clear water layer was sucked out. After drying 12 h, the small loessparticles (LoP) was obtained.

Preparation of PBiNw@LoP

First, 0.388 g dispersants (PVP-K30), 0.158 g BiCl$_3$ and 0.057 g thiourea were dispersed in 35 mL ethylene glycol. Then, 5.0 g LoP was added in mixed solution under stirring at room temperature for 30 min. The mixture was moved into a 50 mL stainless steel reactor, and reacted at 140 °C for 8 h. After the system was gradually cooled down and reached to the ambient temperature, a black granular product was obtained by centrifugation, and washed with acetone and distilled water for several times, respectively. Finally, a granular photocatalyst (PBiNw@LoP) was obtained at 60 °C by vacuum drying for 8 h.

Characterization

The mineralogical composition and crystalline phase structure were measured by X-ray diffraction (XRD) using Cu Kα radiation at 40 kV, 40 mA and a step size of 0.02° in the range of 5 ~ 80°.Fourier transform infrared spectroscopy (FTIR) spectra were recorded between 4000 and 400 cm^{-1} through the KBr method with a FTS-3000 spectrophotometer. The morphology and size were observed by using ascanning electron microscope (SEM) (ULTRA Plus, at 5 kV, Germany).Micromeritics ASAP 2020 was used to obtain adsorption-desorption isotherms of N$_2$.The specific surface area was determined from the adsorption isotherm by the multipoint Brunauer−Emmet−Teller (BET) method, and the pore size distribution was determined from the desorption isotherm by the Barrett−Joyner−Halenda (BJH) method.

Photocatalytic activity

The photoreactivity of the obtained catalyst was evaluated by photodegradation of methylene blue (MB), one of typical dyes, under solar light, and xenon lamp simulated sunlight using a 800 W high-pressure xenon lamp, respectively. Typically, 0.05 g PBiNw@LoP was added to 50 mL of MB solution ([MB]: 20 mg/L). After stirring for 20 min in the dark, the adsorption- desorption equilibrium of MB was established, and then degrade MB under light. At set intervals, the samples were withdrawn from the reactor and filtered by PES syringe filter (pore size: 0.22 μm) for removal of photocatalyst particles. Finally, the UV spectrophotometer is used to determine the absorbance of the solution at 664 nm.

Results and Discussion

Recently, the loess had been paid attention as materials since its friendly environment, cheap availability and special surface texture[22,23], and it had been applied to produce and manufacture as building materials[24], humidity conditioning materials[25], soil and water conservation[26,27]. We found that loess could be used to prepare polymer adsorbent for removing lead ions[28]. In this paper, the small LoP were separated for the first. Then, using LoP, a kind of extremely common and inexpensive natural silicate particles with metastable structure, as inorganic carrier, the petaloid Bi$_2$S$_3$nanowires loaded onloess particles in-situ depositing, which afforded loess particles loaded petaloid Bi$_2$S$_3$nanowires (PBiNw@LoP). After being characterized by SEM, FTIR, XRD etc., its photocatalytic properties were investigated by photodegradation of a typical dye (MB) under solar light.

Chacterizations

The surface morphology of PBiNw@LoP and its materials (LoP) were observed by SEM techinque. As shown in Fig. 1a, LoP were irregular particles, and there shapes are bar, sheet and blocky with size being 1~8 μm. In PBiNw@LoP, the petaloid Bi$_2$S$_3$ nanowires was loaded on LoP particles, and the size of Bi$_2$S$_3$ nanowires is uniform with 20 nm of diameter and 1 μm of length as shown in Fig. 1b. That means the petaloid Bi$_2$S$_3$ nanowires was synthesized[29] and successfully loaded on the loose and multi crevice surface of loess particles. The petaloid Bi$_2$S$_3$ nanowires have a larger specific surface area. The loose and multi crevice loess particles have strong adsorption properties, and they are synergistic. Therefore, the absorption of light is enhanced.

FTIR spectra of PBiNw@LoP, petaloid Bi_2S_3 nanowires, and LoP were depicted in Fig. 2. The characteristic band near 1300~1400 cm^{-1} is the stretching vibration of the Bi-S band in PBiNw@LoP[30]. The characteristic peak in the vicinity of 490 cm^{-1} can be indexed to the bending vibration of Si-O-Si in LoP. The characteristic peak near 1084 cm^{-1} is related to the stretching vibration of Si-O-Si in the loess area. The wide absorption peak near 3300~3600 cm^{-1} is attributed to the stretching vibration of the hydroxyl (O-H) on the surface of the loess. It is clear that the structure of loess particles is basically maintained, and the characteristic peaks of Bi_2S_3 can also be detected. It indicates that the composite material is composed of loess particles and Bi_2S_3, which is consistent with the SEM results.

The XRD diagram of LoP, PBiNw@LoP, and petaloid Bi_2S_3 nanowires are shown in Fig. 3. In PBiNw@LoP, the diffraction peaks at 25° and 27° belong to the characteristic diffraction peak of petaloid Bi_2S_3 nanowires. The diffraction peaks at 26°, 50°, 60° and 68° is the characteristic diffraction peak of quartz in the loess. The diffraction peak at the position 28° is the characteristic diffraction peak of amorphous silicate or aluminosilicate in the loess. In PBiNw@LoP the strongest peak of at 27° was analysed by Scherer equation (Eqn 1).

$$D_{hkl}= 0.89\lambda / \beta_{hkl}\cos\theta \qquad \ldots (1)$$

Where D_{hkl} is the size of crystal (nm); θ is Bragg angle and β_{hkl} is the half peak width (FMHM).

After deducting the background, and using the half-peak width (0.136), the average size of PBiNw@LoP was calculated, and the result was 59.0 nm, which was consistent with the electron microscope results. It indicates that the composite is made up of loess and Bi_2S_3, and the addition of Bi_2S_3 does not destroy the original molecular structure of the loess.

The nitrogen adsorption-desorption isotherm curves were used to analyze the specific surface area of PBiNw@LoP. N_2 adsorption/desorption isotherms of LoP, PBiNw@LoP, and petaloid Bi_2S_3 nanowires (Fig. 4) are shown that they are macroporous materials. They showed adsorption type-S isotherm with H3 type hysteresis loop on relative pressure (P/P$_0$). The adsorption performance of PBiNw@LoP is the best, followed by LoP and petaloid Bi_2S_3 nanowires. Surface area, pore size, and pore volume of LoP, PBiNw@LoP, and petaloid Bi_2S_3

nanowiresare shown in Table 1. The specific surface area, pore volume, and pore size of PBiNw@LoP are largest which is in agreement with the SEM diagram. The loose and porous surface of PBiNw@LoP presents a larger specific surface area. Therefore, it was beneficial to adsorb the dye on the surface of the material, and thus degraded it more effectively.
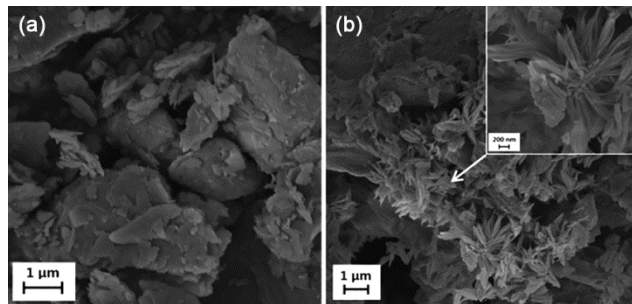

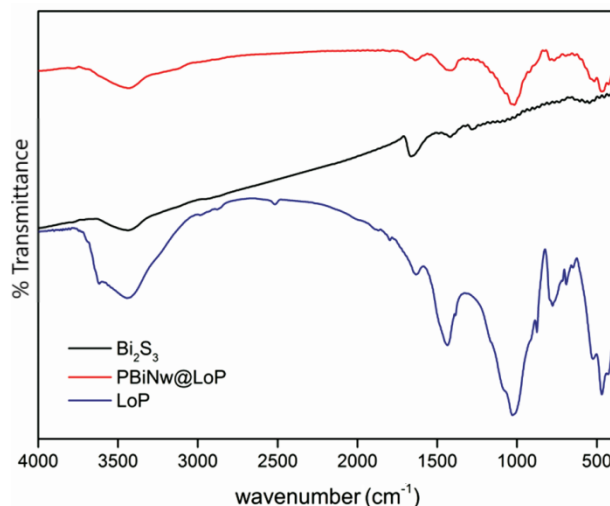Fig. 1 — The SEM micrographs of (a) LoP and (b) PBiNw@LoP.

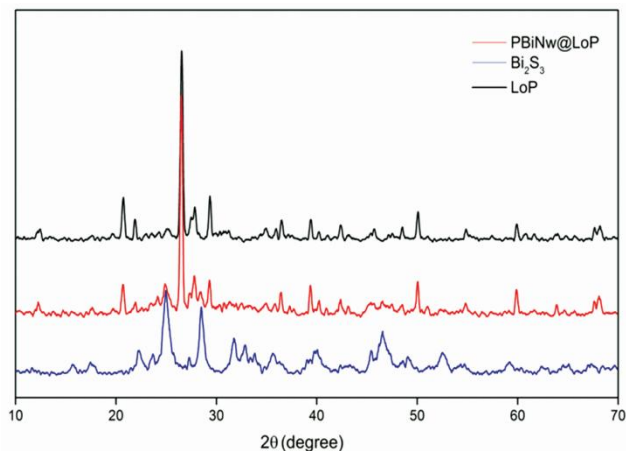Fig. 2 — FTIR spectra of LoP, Bi_2S_3 and PBiNw@LoP.

Fig. 3 — The XRD patterns of LoP, Bi_2S_3 and PBiNw@LoP.

Photocatalytic performance for degradation of dyes

The photocatalytic performance of the catalyst was determined by photodegradation of MB, a typical dye. Take a group of MB solutions (20 mg/L) with volume of 50 mL, 0.05 gPBiNw@LoP was added. Dark reaction for 20 min at room temperature, and then light irradiated for 70 min. According to the obtained results (Fig. 5), at the end of the dark reaction, the degradation rate of pure petaloid Bi$_2$S$_3$ nanowires reached 32.45%, while the degradation rate of PBiNw@LoP reached 58.40%. At 30 min, the pure petaloid Bi$_2$S$_3$nanowires has basically reached thebest degradation performance, and the degradation rate is 77.49%, but when 5 min, the PBiNw@LoP basically reached the upper limit of degradation, and the degradation rate got to 99.50%. As we know, the petaloid Bi$_2$S$_3$ nanowires are a typical photocatalyst for photodegradation dye[31]. Here, compared with reported results[32], the prepared photocatalyst has higher photocatalytic performance and lower cost. These prove that take the petaloid Bi$_2$S$_3$nanowires load on loess particles, the catalytic activity is greatly improved by combine the adsorption of loess particles and the photocatalytic performance of petaloid Bi$_2$S$_3$nanowires. The interaction of the photocatalytic properties of the petaloid Bi$_2$S$_3$ nanowires and the

adsorption properties of the loess make the catalytic degradation rate reach 99.50%. The amount of petaloid Bi$_2$S$_3$ nanowire was reduced without affecting the photocatalytic degradation performance and reducing the cost.

The recyclability of PBiNw@LoP was measured, and the result was shown in Fig. 6. The catalytic performance remains around 90% when the catalyst is reused for 6 times. Repeated use of 7 times, the catalytic activity begins to decrease obviously. At the 10 times, we increase the amount of composite photocatalyst, and the photocatalytic degradation performance reached more than 90% again. Therefore, it was proved that the performance reduction was due to the loss of the catalyst during the repetition process. It can be seen that the prepared catalyst can also be recycled.
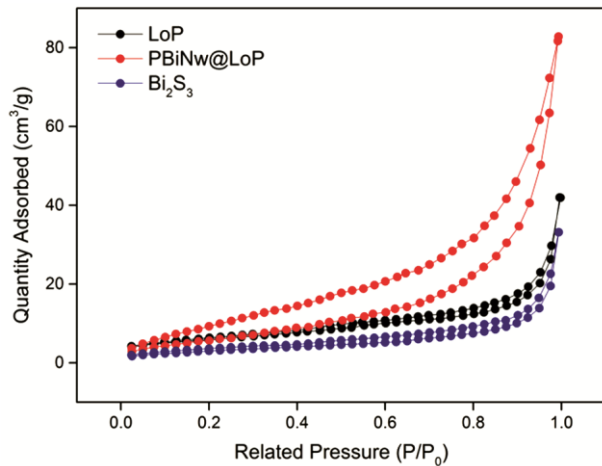

Fig. 4 — N$_2$ adsorption/desorption isotherms of PBiNw@LoP and its materials.

Table 1 — Surface area, pore size, and pore volume of PBiNw@LoP

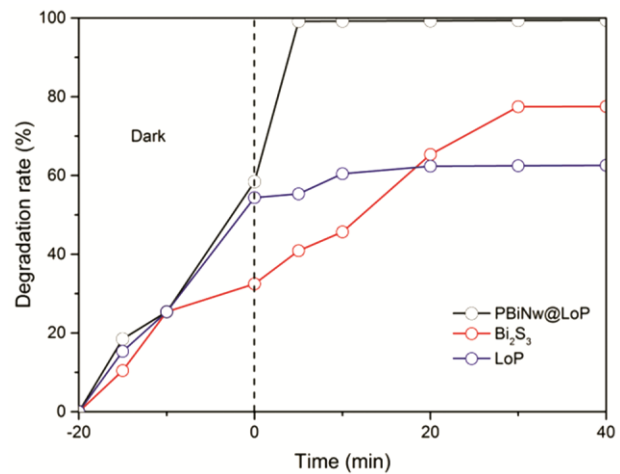|	Surface area (m^{2}g^{-1})	Pore size (nm)	Pore volume (cm^{3}g^{-1})
Bi$_2$S$_3$	10.500	3.712	0.05128
LoP	21.190	12.2313	0.06480
PBiNw@LoP	22.424	17.9506	0.06532

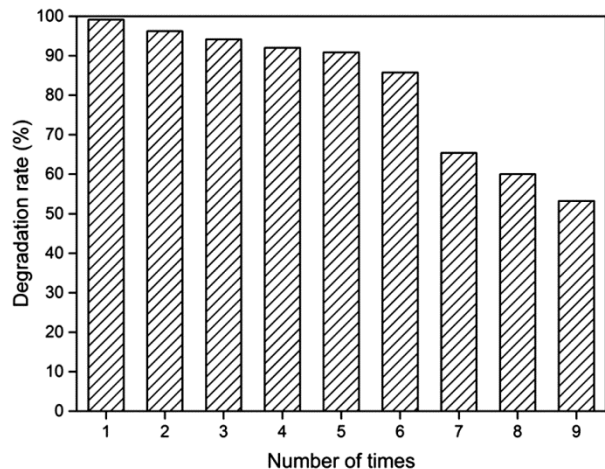Fig. 5 — The degradation performance of LoP, Bi$_2$S$_3$ and PBiNw@LoP.

Fig. 6 — Plot for catalytic degradation performance after repeated experiments.
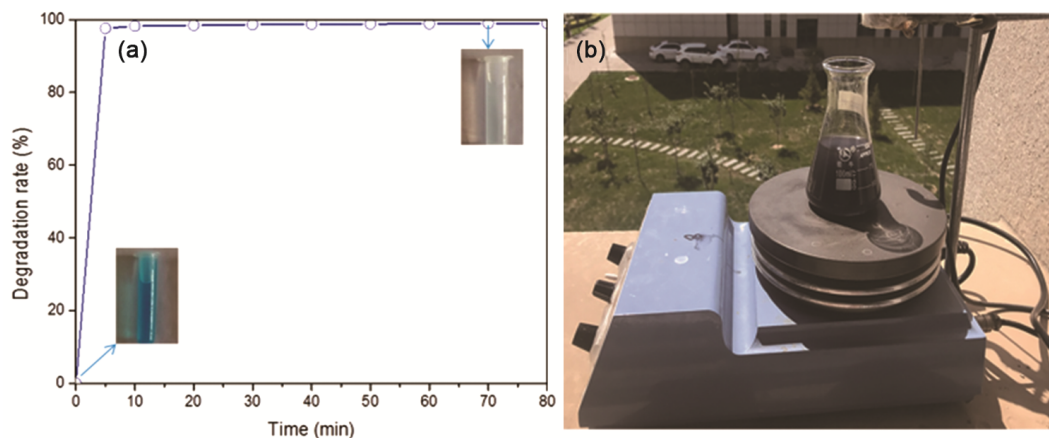
Fig. 7 — Photodegradation effect under (a) natural light and (b) experimental operation diagram of natural photodegradation.

In order to prove that the prepared photocatalyst has practical value, we carried out a group of experiments directly under sunlight. It can be seen from the Fig. 7 that the catalyst has excellent catalytic performance under sunlight. At 5 min, the degradation rate has reached 97.62%. When the reaction lasted for 60 min, the degradation rate reached 98.90%. These prove that the prepared photocatalyst has good photodegradation effect under sunlight and can be applied to real life.

The mechanism of the photocatalytic MB degradation was suggested in Fig. 8. On the surface of catalysts, the adsorbed O_2 reacts with photoelectrons, and produce superoxide anion radicals ($\cdot O^{2-}$). The photoholes left in the VB of Bi_2S_3 will react with H_2O or OH^- to generate hydroxyl radicals[33] ($\cdot OH$). In details, MB binds to the active sites on the PBiNw@LoP surface first by adsorption due to good adsorbability of LoP. Under solar light conditions, electron holes (h^+) are generated on the surface of the photocatalyst, and h^+ further decomposes a series of organic pollutants such as MB through electron capture reduction. At the same time, photogenerated electrons (e^-) can also combine with O_2 in water to generate O^{2-}. After interacting with H_2O molecules[34], the $\cdot O^{2-}$ could produce $\cdot OH$. In addition, O^{2-} can break the covalent bond in MB molecules through oxidation[35], thus achieving the purpose of photocatalytic decomposing of MB into H_2O and CO_2.

In order to investigate photocatalytic mechanism, PBiNw@LoP was measured with UV-visible diffuse reflectance absorption spectra, and the results are shown in Fig. 9. Compared with pristine Bi_2S_3, the absorption intensity of PBiNw@LoP increased obviously. It indicated that PBiNw@LoP
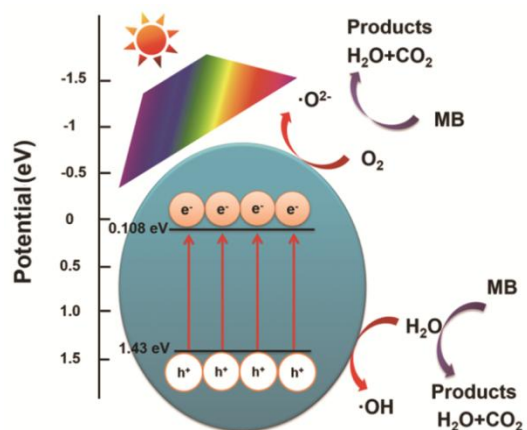

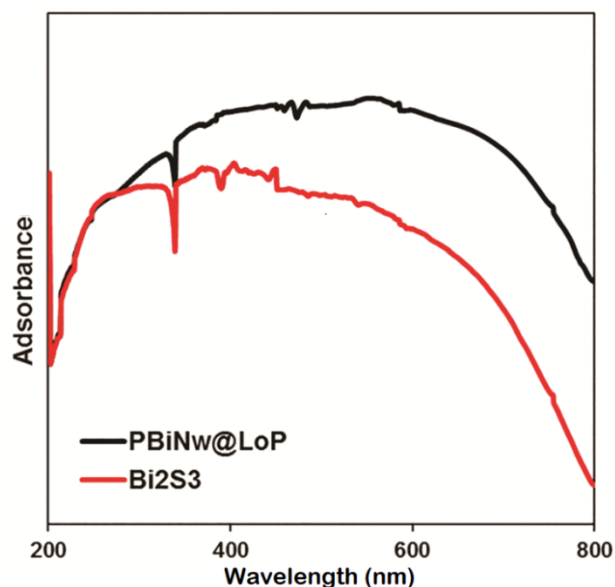
Fig. 8 — Mechanism of the photocatalytic MB degradation.

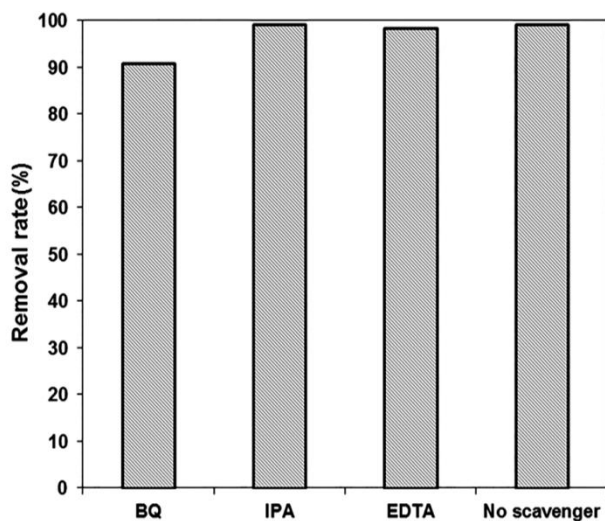Fig. 9 — UV-visible absorption spectra of Bi_2S_3 and PBiNw@LoP.

Fig. 10 — Photodegradation for MB using PBiNw@LoP in the presence of different scavengers.

exhibited better absorption under the UV-visible region, especially under visible light. That means the introduction of Bi$_2$S$_3$ will be in favor of visible light absorption and thus facilitated the full utilization of solar energy. In another side, some inhibitors, such as benzoquinone (BQ), EDTA and IPA, were applied to investigate photocatalytic mechanism, and the results were shown in Fig. 10. Adding IPA, the degradation efficiency changed slightly. That means that •OH is not the key active substance in the photocatalytic reaction system. However, adding BQ or EDTA, the degradation efficiency was obviously inhibited, indicating that •O^{2-} and h$^+$ were the main active substances in the photocatalytic reaction system. The results of UV-visible spectra and active species capture experiments are according with the suggested photocatalytic mechanism.

Conclusions

Loess-based photocatalyst PBiNw@LoP was prepared by a simple one-pot method. The petaloid Bi$_2$S$_3$nanowires are uniformly loaded on the surface of the loess, which not only reduces the use of Bi$_2$S$_3$, but also improves the photocatalytic activity. Loess as a carrier reduces the cost of catalyst, and the loess is not only non-toxic and pollution-free, but also widely exists in nature. The prepared photocatalyst PBiNw@LoP has excellent degradation property fordye and could be good recyclability to use. In summary, a novel eco-friendly photocatalyst based on the loess substrate with good performance and low cost has been successfully prepared, there will be a good prospect for water treatment in the future.

References

1   Liao J, Chen J, Ru X, Wu H & Wei C, *Geochem Explor,* 176 (2016) 9.
2   Cao S, Duan X, Ma Y, Zhao X, Qin Y, Liu Y, Li S, Zheng B & Wei F, *Chemosphere*, 184 (2017) 866.
3   Gil B, Roth W J, Grzybek J, Olejniczak A Z, Elias M, Opanasenko M & Cejka J, *Catal Today*, 304 (2018) 22.
4   Li Y & Yeung K L, *Catal Today*, 331 (2019) 53.
5   Chen K C, Wang Y H & Lu Y C, *Catal Today*, 175 (2011) 276.
6   Kalal S, Chauhan N P S, Pandey A, Ameta R & Punjabi P B . *Indian J Chem,* 54A (2015) 1057.
7   Hisatomi T, Kubota J & Domen K, *Chem Soc Rev,* 46 (2015) 7520.
8   Shintre S N & Thakur P, *Indian J Chem Tech*, 23 (2016) 232.
9   Wang S, Yang Q, Chen F, Sun J, Luo K, Yao F B, Wang X L, Wang D B, Li X M & Zeng G G, *Chem. Eng. J,* 328 (2017) 927.
10 Li D, Shi W, Chinese, *J Catal*, 37 (2016) 792.
11 Lalitha K, Kumari V D & Subrahmanyam M. *Indian J Chem*, 53A (2014).472.
12 Tang C, Zhang Y, Su J, Wang C, Sun R, Zhang J & Li G, *Solid State. Sci,* 51 (2015) 24.
13 Dang Y, Wang Y, Deng Y, Mao L I, Zhang Y & Zhang Z W, *Met Mater Int*, 21 (2011) 216.
14 Zeynali H, S. Mousavi B & Hosseinpour-Mashkani S M, *Mater Lett*, 144 (2015) 65.
15 Wang J, Jin J, Wang X, Yang S, Zhao Y, Wu Y, Dong S & Sun J, *J Colloid Interf Sci*, 505 (2017) 805.
16 Li X, Chen J, Li H, Li J, Xu Y, Liu Y & Zhou J R, *J Nat Gas Chem*, 20 (2011) 413.
17 Ren L Z, Zhang D E, Hao X Y, Xiao X, Gong J Y, Wang M Y & Tong Z,*Funct Mater Lett*, 10 (2017).
18 Luo S, Qin F, Ming Y, Zhao H, Liu Y & Chen R, *J Hazard Mater*, 340 (2017) 253.
19 Long L L, Chen J J, Zhang X, Zhang A Y, Huang Y X &Rong Q, *Npg Asia Mater*, 8 (2016) 263.
20 Bhoi Y P, Mishra B G, *Chem Eng J*, 316 (2017) 70.
21 Ayodhya D, Veerabhadram G, *Superlattice Microst*, 102 (2017) 103.
22 Zhang Z, Wang T, Wu S, Tang H & Liang C, *Eng Geol*, 222 (2017) 225.
23 Zhao X, Li Z, Robeson M D, Hu J & Zhu Q, *Catena*, 160 (2018) 233.
24 Li W, Zhang W Z, Deng D D, Li H M, Wang T & Wang B, *Explor Eng*, 43 (2016) 33.
25 Zhang Y, Jing Z, Fan X, Fan J, Lu L & Ishida E H, *Ind Eng Chem Res*, 52 (2013) 4779.
26 Liu J, Zhang D, Wang Y, Sun M Y & Duan X C, *J Earth Sci,* 38 (2016) 420.
27 Ma G, Ran F, Yang Q, Feng E & Lei Z, *Rsc Adv,* 5 (2015) 53819.

28 He Y, Zhang L, Wang R M, Li H &Wang Y, *J Hazard Mater*, 43 (2012) 334.
29 Wang X, Wei H, Khormali F, Taheri M, Kehl M, Frechen M, Lauer T & Chen F H, *Quatern Int*, 429 (2016) 41.
30 Chen F, Cao Y & Jia D, *J Colloid Interf Sci*, 404 (2013) 110.
31 Kumar S, Sharma S, Umar A & Kansal S K, *Nanosci. Nanotech Let*, 8 (2016) 266.
32 Albuquerque R, Neves M C, Mendonça M H, Trindade T & Monteiro O C, *Colloid Surf A,* 328 (2008) 107.
33 Li B, Zhang Y, Du R, Gan L, & Yu X, *Langmuir,* 32 (2016) 11639.
34 Wang M, Yang L, Yuan J, He L, Song Y, Zhang H, Fang S, *RSC Adv*, 8 (2018) 12459.
35 Tanveer M, Wu Y, Qadeer M A & Cao C, *Sci China Mater,* 61 (2017) 101.